Discovery of a novel SHP2 allosteric inhibitor using virtual screening, FMO calculation and molecular dynamic simulation

Zhen Yuan
East China University of Science & Technology
Manzhan Zhang
East China University of Science & Technology
Longfeng Chang
East China University of Science & Technology
Xingyu Chen
East China University of Science & Technology
Shanshan Ruan
East China University of Science & Technology
Shanshan Shi
East China University of Science & Technology
Yiqing Zhang
East China University of Science & Technology
Lili Zhu
East China University of Science & Technology
Honglin Li
East China University of Science & Technology
Shiliang Li
slli403@163.com

East China University of Science & Technology

Research Article

Keywords: SHP2, allosteric inhibitor, fragment molecular orbital method, virtual screening, molecular dynamics simulation

Posted Date: November 8th, 2023

DOI: https://doi.org/10.21203/rs.3.rs-3565398/v1

Additional Declarations: No competing interests reported.

Version of Record: A version of this preprint was published at Journal of Molecular Modeling on April 13th, 2024. See the published version at https://doi.org/10.1007/s00894-024-05935-y.

Abstract

Investigating the role of protein tyrosine phosphatase SHP2 is a continuing concern in the context of various human diseases, including Noonan syndrome, LEOPARD syndrome, and cancers. SHP2 is an essential bridge to connect numerous oncogenic cell-signaling cascades including RAS-ERK, PI3K-AKT, JAK-STAT and PD-1/PD-L1 pathways. This study aims to discover novel and potent SHP2 inhibitors using a hierarchical structure-based virtual screening strategy that combines molecular docking and the fragment molecular orbital method (FMO) for calculating binding affinity (referred to as the Dock-FMO protocol). We employed Dock-FMO virtual screening of ChemDiv database of ∼2,990,000 compounds to identify a novel SHP2 allosteric inhibitor bearing hydroxyimino acetamide scaffold. Experimental validation demonstrated that the new compound (E)-2-(hydroxyimino)-2-phenyl-N-(piperidin-4-ylmethyl)acetamide (**7188-0011)**effectively inhibited SHP2 in a dose-dependent manner. Molecular dynamics (MD) simulation analysis revealed the binding stability of compound **7188-0011**and the SHP2 protein, along with the key interacting residues in the allosteric binding site. Overall, our work has identified a novel and promising allosteric inhibitor that targets SHP2, providing a new starting point for further optimization to develop more potent inhibitors.

1. Introduction

Src homology-2-containing protein tyrosine phosphatase 2 (SHP2), the first oncogenic non-receptor protein tyrosine phosphatase to be identified, is encoded by the proto-oncogene *PTPN11*. It plays a critical role in various cellular processes including growth, proliferation, differentiation, migration, and apoptosis[1]. SHP2 is comprised of four distinct domains, namely two tandem Src homology 2 domains (N-SH2 and C-SH2), a conserved PTP catalytic domain, and a C-terminal tail housing two tyrosine phosphorylation sites (Tyr542 and Tyr580)[2]. Accumulated evidence has demonstrated that SHP2 actively participates in numerous oncogenic cell-signaling pathways, which encompass RAS-ERK, PI3K-AKT, and JAK-STAT, situated downstream of several receptor tyrosine kinases (RTKs)[1,3–6]. Moreover, it has been reported that SHP2 is involved in the downstream signal transduction of the immunosuppressive receptor PD-1 within the PD-L1/PD-1 pathway, resulting in the suppression of T cell activation[7–9]. SHP2 has been shown to serve dual roles, functioning either as an oncogenic factor or as a tumor suppressor. Dysregulation of SHP2 contributes to a variety of sporadic hematological malignancies, developmental disorders, and solid tumors[10–12]. This extensive range of diseases highlights the potential of SHP2 as a promising target for cancer treatment, leading to substantial interest in SHP2 inhibitors as prospective agents for inhibiting tumor growth.

Over the last two decades, an effort has been devoted to discovering active site inhibitors in the highly conserved catalytic PTP domain[13–16]. Nevertheless, these inhibitors have not advanced to clinical applications owing to challenges associated with poor oral bioavailability, low selectivity, and poor membrane permeability. Until recently, the first allosteric inhibitor (**SHP099**) of SHP2 was reported to stabilize SHP2 in an auto-inhibited conformation that blocks the access of substrates, resulting in

suppressed PTP activity[17]. At present, eight allosteric inhibitors of SHP2 exhibiting high selectivity and oral bioavailability (TNO155, JAB-3068, BBP-398, ERAS-601, JAB-3312, SH3809, RMC-4630, and HBI-2376) have progressed to clinical trials.[10] SHP2 allosteric inhibitors were designed to overcome the poor druggability drawbacks of catalytic site inhibitors and exhibit high therapeutic potential for cancer treatment. In this study, we utilized Dock-FMO virtual screening to identify novel compounds targeting the SHP2 allosteric site. The top-ranked compounds were subsequently selected for biological testing. Among them, compound **7188-0011**, possessing a unique structure, exhibited moderate enzymatic potency. To evaluate the dynamic behavior and binding stability of the **7188-0011**-SHP2 complex, molecular dynamics (MD) simulations further performed.

2. Methods and Materials

2.1 Virtual screening

The crystal structure of SHP2 was obtained from the Protein Data Bank with the accession code 5EHR, of which the resolution is 1.7 Å. The coactivators, as well as all water molecules, were removed from the structure. Hydrogen atoms and charges were added using the Protein Preparation Wizard module in Maestro (Schrödinger Inc, version 10.1). The crystal structure, after optimization of the hydrogen bond network, was subjected to energy minimization using the OPLS3 force field. The grid-enclosing box was placed on the center of the crystallographic ligand and defined to encompass residues within a 15 Å radius around the ligand, constituting the binding pocket. The remaining settings were kept at their default values. Under conditions of pH ranging from 5.0 to 9.0, the addition of hydrogen atoms and ionization facilitated the generation of stereoisomers and 3D conformers for compounds housed within the ChemDiv database (~2,990,000 compounds), employing the Ligprep v3.3 module. Utilizing both the Glide standard precision (SP) and extra precision (XP) methods[18, 19], molecular docking was performed with default parameters, retaining only the highest-ranked pose for each molecule. After Glide SP scorings, the top 15,215 ranked molecules were retained for subsequent calculations using the more precise Glide XP scoring function. Finally, the top-ranked 1,520 molecules were retained for further visual observation. Based on the Tanimoto similarity metric, a hierarchical clustering method was employed to cluster the 1,520 MOLPRINT2D fingerprint features into 25 groups. Taking into consideration ligand binding poses, structural diversity, and novelty, 25 candidates were selected from the pool of 1,520 compounds and subsequently subjected to activity testing.

2.2 Fragment molecular orbital (FMO) calculation

Structure preparation. Prior to the FMO calculation, the complex structures of the ligands and SHP2 were prepared by the Molecular Operating Environment (MOE, version 2014.09). All binding modes of SHP2-ligand complexes in this report were derived from crystallography and molecular docking simulations. The ligand and residues around 4.5 Å of the ligand were cut off into the entire system researched. Hydrogen atoms were added to the complex structure and ionization states of the acidic and basic amino acid residues were assigned with the Protonate 3D tool implemented in MOE applied by default settings

(pH = 7.0, a solvent dielectric constant of 80). Then, the structures were performed energy minimization using the semiempirical Amber10: EHT forced field. During this process, a constraint was applied, restricting each atom from deviating no more than 0.5 Å from its original position, a parameter enforced by the MOE program. We fragmented the entire optimized system using Facio (version 19.1.5) to prepare the FMO input files.

FMO method and inter-fragment interaction energy (IFIE). The FMO method was employed to partition a complex biological system, such as a protein, into smaller parts referred to as fragments, typically corresponding to individual residues. This approach saves a large amount of computation time compared to the traditional quantum mechanical (QM) methods[20, 21]. Generally, the FMO calculation contains the following steps: (1) partition a large system into multiple smaller fragments, (2) iteratively perform Ab initio calculations on each individual fragment (referred to as monomers) within the context of an embedding polarizable potential generated by the surrounding fragments until self-consistency is achieved in the electron densities, (3) calculate self-consistent field (SCF) of fragment pair, introducing interfragment charge transfer along with other quantum effects into the calculations, (4) calculate the total energy of the system.

In our calculation, all FMO calculations were performed using General Atomic and Molecular Electronic Structure System (GAMESS, version Sep, 2020) [22, 23] and were performed by second-order Møller-Plesset perturbation (MP2) methods with the 6-31G* basis set (FMO-MP2/6-31G*). We treated the amino group as neutralized residue to avoid overestimating charge-charge interactions due to calculations in vacuum conditions. The FMO-based IFIE between fragment i and j, $\Delta E_{ij}^{\mathrm{int}}$, is given by

$$\Delta E_{ij}^{\mathrm{int}} = \Delta E_{ij}^{\mathrm{ES}} + \Delta E_{ij}^{\mathrm{EX}} + \Delta E_{ij}^{\mathrm{CT+MIX}} + \Delta E_{ij}^{\mathrm{DI}}$$

Where $\Delta E_{ij}^{\mathrm{ES}}$,$\Delta E_{ij}^{\mathrm{EX}}$,$\Delta E_{ij}^{\mathrm{CT+MIX}}$and $\Delta E_{ij}^{\mathrm{DI}}$represent the electrostatic, exchange repulsion, charge transfer with higher-order mixed and dispersion terms, obtained by the pair interaction energies decomposition analysis (PIEDA)[24].

2.3 Molecular dynamics simulation

In order to investigate the stability and behavior of the **7188-0011**-protein complex, molecular dynamics (MD) was performed using AmberTools18 simulation package (University of California, San Francisco, CA, USA) for 100 ns. The parameters file was generated for protein using the FF14SB forcefield, while the corresponding ligand parameters file was generated using antechamber and parmchk modules in AmberTools18. Subsequently, the complex was neutralized by adding appropriate counter ions (Cl^-) and was solvated in a cubic box using TIP3PBOX water molecule with the box's edge at least 1.0 nm away from the complex. Energy minimization was achieved by employing the steepest-descent algorithm for 5000 steps, which was subsequently followed by the conjugate-gradient algorithm for an additional 5000 steps. Subsequently, pre-equilibration took place in two sequential steps, comprising a constant NVT ensemble (maintaining a constant particle number, volume, and temperature) and a constant NPT

ensemble (maintaining a constant particle number, pressure, and temperature). The former indicates that the simulation system was heated up progressively from 0 to 300 K for 200 ps using *Langevin* thermostat, and the latter was used to perform pressure equilibration for 100 ps at 300K using *Berendsen* barostat. Finally, the position restraint was removed, and the production run was carried out for 100 ns with a 2 fs step. The RMSD, RMSF, H-bonds, and cluster analysis were calculated with *cpptraj* utility in AmberTools18. Furthermore, the binding energy of the complex was estimated for 250 snapshots using MM/GB(PB)SA methods implemented in the mmpbsa.py tool of AmberTools18.

2.4 Biochemical assay

The gene encoding human $SHP2^{WT}$ (1-593) and $SHP2^{PTP}$ (237–529) were inserted into the pET30 vector respectively. Two proteins were purified and expressed as described previously in the literature[25]. The allosteric activation of SHP2 was observed upon the binding of a phosphorylated peptide containing bis-tyrosyl to its Src homology 2 (SH2) domain. This activation process leads to the liberation of the inhibitory interface of SHP2, thereby enabling the accessibility of its PTP domain for substrate identification and catalysis. The rapid fluorescence assay was employed to detect the catalytic activity of SHP2, utilizing DiFMUP as a surrogate substrate. The experimental reagents prepared were as follows: 12.5 μL of buffer (75 mM NaCl, 75 mM KCl, 60 mM HEPES, pH 7.2, 1 mM EDTA, 0.05% P-20, 5 mM DTT), 2.5 μL of peptide IRS1_pY1172 (dPEG8) pY1222 (Shanghai Shengzhao Biotech Co., Ltd. cat. no. 79319-2), 2.5 μL of test compound, 2.5 μL of $SHP2^{WT}$ or $SHP2^{PTP}$. And 20 μL reaction buffer was added to the 384-well plate (Perkin Elmer, cat. no. 6008260) and incubated for one hour at ambient temperature. Afterwards, the reaction was initiated by adding 200 μM surrogate substrate DiFMUP (Invitrogen, cat. no. D6567), followed by incubation at 25°C for an additional 30 minutes. Subsequently, a 5 μL solution containing bpV(Phen) with a concentration of 160 μM (Enzo Life Sciences cat# ALX-270-204) was added to halt the reaction. The fluorescence signal was then monitored by exciting the sample at 340 nm and measuring the emitted light at 450 nm. The inhibition rates were calculated by measuring the percentage of dephosphorylation of DiFMUP catalyzed by the enzyme. For each inhibitor, seven different concentrations were used to determine the IC_{50}. **SHP099** (Guangzhou Qiyun Biotechnology Co., Ltd., cat. no.1801747-42-1) was used as the positive control. Each experiment was performed at least three parallels.

3. Results and Discussion

3.1 Construction of Dock-FMO virtual screening protocol

According to the previous report[26–30], the fragment molecular orbital (FMO) method, developed by Kitaura and co-workers[20, 21, 31], can achieve high precision to predict a complete list of the pair interaction energy (PIE) to study ligand – protein interactions by performing ab initio quantum-chemical calculations for biomolecular systems. Therefore, the FMO calculation for predicting intermolecular interactions is recognized as a reliable method for calculating binding energies with satisfactory accuracy, but this method was limited to computational cost and is not suitable for large-scale virtual screening purposes.

In order to improve hit rates, this study incorporated the FMO method as a high-precision binding affinity prediction step following the traditional virtual screening workflow, resulting in a approach known as the Dock-FMO virtual screening method.

Prior to the virtual screening, the Dock-FMO protocol was validated by redocking and correlation analysis between FMO-based interaction energies and the experimental binding free energies. Initially, pose validation was carried out by redocking the co-crystallized ligand into the allosteric site of SHP2 (PDB: 5EHR). The RMSD between the co-crystallized conformation and the best pose docked by Glide SP is 0.574 Å, which indicates that the Glide SP can predict active conformation of the ligand. Next, to investigate the prediction accuracy of the FMO method for calculating protein-ligand interactions of the SHP2 target, we manually curated a dataset including 51 ligand structures and affinities (IC_{50}) from papers[17, 25, 32–35] (**Table S1**). The sums of PIEs between 51 ligands with diverse chemical scaffolds and the SHP2 protein correlated well with their biological potencies (R^2 = 0.55, Fig. 1A **and Supplemental Data**). Comparing FMO results on this dataset with results for MM/PBSA and MM/GBSA (R^2 = 0.02 and 0.15, respectively, Fig. 1A **and Supplemental Data**), we found that FMO method showed a higher correlation to experimental data. Therefore, the FMO analysis was employed as a critical strategy to determine the binding affinities between ligands and proteins.

3.2 Virtual screening and compounds selection

To identify the key residues in the SHP2 allosteric site, we performed FMO calculations and PIEDA analysis. We calculated the interaction energies between **SHP099**, a lead compound, and the surrounding residues of SHP2 protein (PDB:5EHR) using the FMO method to understand the ligand binding mechanism of SHP2. The interaction energies of R111 and E250 have high ES and CT + MIX terms calculated from the PIEDA analysis (**Figure S1 and Table S2**), indicating they could form hydrogen bonds with the ligand. In addition, E249 and H114 could form a salt bridge with SHP099, as indicated by their high contributions in ES and CT + MIX terms. Furthermore, L254 and P491 could form hydrophobic and CH/π interactions with DI term contribution (-3.0 ~ -7.2 kcal/mol). As indicated by the PIEDA analysis, E250 (PTP), E249 (PTP), R111 (N-SH2), and H114 (N-SH2) are identified as key residues involved in ligand binding at the SHP2 allosteric site. The result provides a reliable reference for subsequent virtual screening research.

In order to identify potent SHP2 allosteric inhibitors, we first carried out the Dock-FMO virtual screening protocol against the ChemDiv database (~2,990,000 compounds), followed by in vitro activity assays, as shown in Fig. 1B. All compounds were filtered by Lipinski's rule of five, PAINS (pan assay interference filters), and ADME/T calculated by the Qikprop module. After successively docking and scoring by high throughput virtual screening (HTVS), Glide SP, and Glide XP, the remaining compounds were then grouped into 25 clusters based on the Tanimoto similarity metric. After individually checking these compounds for the formation of critical interactions, we selected 39 compounds for further evaluation by FMO analysis. The top 60% of compounds ranked by binding affinities (25 compounds, whose sum of PIE was lower than − 85 kcal/mol) were further selected and purchased for biochemical assays (**Table S3**).

3.3 In vitro biological activity

After a hierarchical structure-based virtual screening of the SHP2 protein, we obtained 25 candidate compounds to test for the SHP2 enzyme activity. In this study, we built a fluorescence-based phosphatase biochemical assay was built to assess the dephosphorylation of 6,8-difluoro-4-methylumbelliferyl phosphate (0.5 μM 2P-IRS-1, DIFMUP assay[35]) as a means of validating SHP2 allosteric inhibitors. SHP099 reported by Novartis[17] was used as the positive control ($SHP2^{WT}$ IC_{50} = 0.078 μM, $SHP2^{PTP}$ IC_{50} > 100 μM), and the data was broadly consistent with the experimental value reported previously[17]. Therefore, we established the SHP2 allosteric inhibitor screening system. As shown in Fig. 2A, the 25 tested compounds were initially screened against SHP2 full length ($SHP2^{WT}$) at 50 μM, and 1 hit (**7188-0011**, Fig. 2A) with 52% of inhibitory rate was further validated by the $SHP2^{PTP}$ -based dephosphorylation assay ($SHP2^{PTP}$ IC_{50} > 100 μM), which indicated that the inhibitor could not bind to the PTP active site. The positive control (0.1 μM **SHP099**) showed 65% inhibition. The hit compound effectively inhibited the activity of $SHP2^{WT}$ with the IC_{50} value of 54.31 ± 0.67 μM (Fig. 2B).

3.4 Binding mode analysis

The predicted binding mode of **7188-0011** showed a similar pattern to the observed **SHP099** binding mode in the crystal structure (Fig. 3A **and Figure S2**). FMO analysis of **7188-0011** revealed 5 key interactions with SHP2 (Fig. 3A). The inhibitor is positioned in a narrow polar pocket between PTP, C-SH2, and N-SH2 domains of SHP2. PIEDA results indicated that the inhibitor could form hydrogen bonds with E250 and R111 and could form a salt bridge with E249, which have high ES and CT + MIX terms contribution (Fig. 3C). These residues played important roles in molecular recognition. In addition, T253, L524, and P491 could form CH/π interactions with the inhibitor, which have slightly high DI term contribution. The PIEDA results indicated that the binding mode of **7188-0011** and **SHP099** are consistent, suggesting that **7188-0011** exerts its inhibitory function by interacting with the same key residues of the protein. Therefore, the binding stability of **7188-0011** to the protein was next explored using molecular dynamics (MD) simulations.

3.5 MD simulations

MD simulations have been regarded as a vital computational tool to investigate the time-dependent stability of ligands in the active site of proteins. The binding stability of the hit compound (**7188 – 1100**) was further evaluated by performing MD simulations for 100 ns. The RMSD of backbone atoms of the complex and the apo structure (without ligand) were plotted in Fig. 4A. The backbone of the complex and the apo structure reached equilibration at about 30 ns and then stabilized, oscillating around the 2 Å value. Meanwhile, we computed the root-mean-square fluctuation (RMSF) of all residues after the 30 ns simulation to assess both ligand deviation from the initial conformation and the extent of residue movement in SHP2 in both the unbound state and upon ligand binding. (Fig. 4B). The RMSF value for the free protein and the protein involved in the complex displayed a constant trend, but these overall

fluctuations were minimized in the binding state in general. These results further indicated that the ligand could enhance the stability of protein during the simulation. The detailed analysis revealed that strong hydrogen bond interactions were found between the ligand and residues E250 and F113, kept for 93.64% and 62.22%, respectively. The π-cation interaction and hydrogen bond interactions were found between the **7188-0011** and R111 (Fig. 4C-4D). However, the high flexibility of the **7188-0011** compound itself, as well as its inadequate hydrophobicity at the head region (phenyl), was considered to be the reasons for its poor activity. This could potentially be a promising direction for future hit optimization to improve affinity with the target.

4. Conclusion

SHP2, a protein tyrosine phosphatase, has emerged as a therapeutic target for various human diseases, particularly cancer. In this study, we employed a rigorous virtual screening method called Dock-FMO, including molecular docking for primary screening and FMO methods for binding affinity calculation. Therefore, to identify potent SHP2 allosteric inhibitors, we carried out the Dock-FMO virtual screening protocol against the ChemDiv database. Subsequently, the 25 compounds were selected for in vitro activity assays, and experimental validation revealed that compound **7188-0011** inhibited SHP2 in a dose-dependent manner (IC_{50} = 54.31 ± 0.67 μM). MD simulations further confirmed the high binding stability between **7188-0011** and SHP2 protein. This study provided a novel and promising allosteric inhibitor, laying the foundation for the development of anti-tumor drugs targeting the SHP2 protein. It also serves as the basis for further lead compound optimization to develop more active inhibitors.

Declarations

CRediT authorship contribution statement

Zhen Yuan: Methodology, Investigation, Data curation, Visualization, Writing – original draft, Writing – review and editing. **Manzhan Zhang:** Methodology, Investigation, Writing – original draft. **Longfeng Chang:** Resources, Validation. **Xingyu Chen**: Data curation. **Shanshan Ruan:** Data curation, **Shanshan Shi:** Data curation, **Yiqing Zhang:** Data curation. **Lili Zhu:** Writing – review and editing, Supervision, Funding acquisition. **Honglin Li:** Conceptualization – review and editing, Supervision, Funding acquisition. **Shiliang Li:** Conceptualization, Writing – review and editing, Supervision, Funding acquisition. All authors have read and agreed to the published version of the manuscript.

Declaration of Competing Interest

The authors declare that they have no known competing financial interests or personal relationships that could have appeared to influence the work reported in this paper.

Funding

This work was supported in part by the National Key R&D Program of China (2022YFC3400501, 2022YFC3400504); the National Natural Science Foundation of China (grants 82173690 to S.L.L., 81825020 and 82150208 to H.L.,); the Lingang Laboratory (grant LG-QS-202206-02 to S.L.L.); the Fundamental Research Funds for the Central Universities; S.L.L. is also sponsored by the Shanghai Rising-Star Program (23QA1402800). Honglin Li was also sponsored by the National Program for Special Supports of Eminent Professionals and National Program for Support of Top-Notch Young Professionals.

Appendix A. Supplementary material

The Supporting Information to this article can be found in the online version. Results of Dock-FMO virtual screening and biochemical assay; information for the binding mode analysis of **SHP099**; PIEDA analysis for ligands (**SHP099** and **7188-0011**) and the surrounding residues with FMO method. Supplementary data of a dataset for testing the performance of FMO calculation, MM/PBSA and MM/GBSA as csv files.

References

1. Chan, R. J.; Feng, G. S., PTPN11 is the first identified proto-oncogene that encodes a tyrosine phosphatase. *Blood.* **2007,** *109* (3), 862-7.
2. Barr, A. J.; Ugochukwu, E.; Lee, W. H., et al., Large-scale structural analysis of the classical human protein tyrosine phosphatome. *Cell.* **2009,** *136* (2), 352-63.
3. Neel, B. G.; Gu, H.; Pao, L., The 'Shp'ing news: SH2 domain-containing tyrosine phosphatases in cell signaling. *Trends in biochemical sciences.* **2003,** *28* (6), 284-93.
4. Tiganis, T.; Bennett, A. M., Protein tyrosine phosphatase function: the substrate perspective. *The Biochemical journal.* **2007,** *402* (1), 1-15.
5. Vazhappilly, C. G.; Saleh, E.; Ramadan, W., et al., Inhibition of SHP2 by new compounds induces differential effects on RAS/RAF/ERK and PI3K/AKT pathways in different cancer cell types. *Investigational new drugs.* **2019,** *37* (2), 252-261.
6. Wong, G. S.; Zhou, J.; Liu, J. B., et al., Targeting wild-type KRAS-amplified gastroesophageal cancer through combined MEK and SHP2 inhibition. *Nature medicine.* **2018,** *24* (7), 968-977.
7. Gavrieli, M.; Watanabe, N.; Loftin, S. K., et al., Characterization of phosphotyrosine binding motifs in the cytoplasmic domain of B and T lymphocyte attenuator required for association with protein tyrosine phosphatases SHP-1 and SHP-2. *Biochem. Biophys. Res. Commun.* **2003,** *312* (4), 1236-43.
8. Yokosuka, T.; Takamatsu, M.; Kobayashi-Imanishi, W., et al., Programmed cell death 1 forms negative costimulatory microclusters that directly inhibit T cell receptor signaling by recruiting phosphatase SHP2. *J Exp Med.* **2012,** *209* (6), 1201-17.
9. Chemnitz, J. M.; Parry, R. V.; Nichols, K. E., et al., SHP-1 and SHP-2 associate with immunoreceptor tyrosine-based switch motif of programmed death 1 upon primary human T cell stimulation, but only receptor ligation prevents T cell activation. *Journal of immunology (Baltimore, Md. : 1950).* **2004,** *173* (2), 945-54.

10. Song, Y.; Zhao, M.; Zhang, H., et al., Double-edged roles of protein tyrosine phosphatase SHP2 in cancer and its inhibitors in clinical trials. *Pharmacol Ther.* **2022,** *230*, 107966.
11. Miyamoto, D.; Miyamoto, M.; Takahashi, A., et al., Isolation of a distinct class of gain-of-function SHP-2 mutants with oncogenic RAS-like transforming activity from solid tumors. *Oncogene.* **2008,** *27* (25), 3508-15.
12. Chan, G.; Kalaitzidis, D.; Neel, B. G., The tyrosine phosphatase Shp2 (PTPN11) in cancer. *Cancer Metastasis Rev.* **2008,** *27* (2), 179-92.
13. Grosskopf, S.; Eckert, C.; Arkona, C., et al., Selective inhibitors of the protein tyrosine phosphatase SHP2 block cellular motility and growth of cancer cells in vitro and in vivo. *ChemMedChem.* **2015,** *10* (5), 815-26.
14. Chen, C.; Liang, F.; Chen, B., et al., Identification of demethylincisterol A(3) as a selective inhibitor of protein tyrosine phosphatase Shp2. *Eur J Pharmacol.* **2017,** *795*, 124-133.
15. Chen, C.; Cao, M.; Zhu, S., et al., Discovery of a Novel Inhibitor of the Protein Tyrosine Phosphatase Shp2. *Sci. Rep.* **2015,** *5*, 17626.
16. Chen, L.; Sung, S. S.; Yip, M. L., et al., Discovery of a novel shp2 protein tyrosine phosphatase inhibitor. *Molecular pharmacology.* **2006,** *70* (2), 562-70.
17. Chen, Y. N.; LaMarche, M. J.; Chan, H. M., et al., Allosteric inhibition of SHP2 phosphatase inhibits cancers driven by receptor tyrosine kinases. *Nature.* **2016,** *535* (7610), 148-52.
18. Friesner, R. A.; Banks, J. L.; Murphy, R. B., et al., Glide: A New Approach for Rapid, Accurate Docking and Scoring. 1. Method and Assessment of Docking Accuracy. *Journal of Medicinal Chemistry.* **2004,** *47* (7), 1739-1749.
19. Halgren, T. A.; Murphy, R. B.; Friesner, R. A., et al., Glide: A New Approach for Rapid, Accurate Docking and Scoring. 2. Enrichment Factors in Database Screening. *Journal of Medicinal Chemistry.* **2004,** *47* (7), 1750-1759.
20. Fedorov, D. G.; Kitaura, K., Extending the power of quantum chemistry to large systems with the fragment molecular orbital method. *The journal of physical chemistry. A.* **2007,** *111* (30), 6904-14.
21. Fedorov, D. G.; Nagata, T.; Kitaura, K., Exploring chemistry with the fragment molecular orbital method. *Phys Chem Chem Phys.* **2012,** *14* (21), 7562-77.
22. Fedorov, D. G., The fragment molecular orbital method: theoretical development, implementation in GAMESS, and applications. *WIREs Computational Molecular Science.* **2017,** *7* (6), e1322.
23. Schmidt, M. W.; Baldridge, K. K.; Boatz, J. A., et al., General atomic and molecular electronic structure system. *Journal of Computational Chemistry.* **1993,** *14* (11), 1347-1363.
24. Fedorov, D. G.; Kitaura, K., Pair interaction energy decomposition analysis. *J. Comput. Chem.* **2007,** *28* (1), 222-237.
25. LaMarche, M. J.; Acker, M.; Argintaru, A., et al., Identification of TNO155, an Allosteric SHP2 Inhibitor for the Treatment of Cancer. *J Med Chem.* **2020,** *63* (22), 13578-13594.

26. Sriwilaijaroen, N.; Magesh, S.; Imamura, A., et al., A Novel Potent and Highly Specific Inhibitor against Influenza Viral N1-N9 Neuraminidases: Insight into Neuraminidase-Inhibitor Interactions. *J Med Chem.* **2016,** *59* (10), 4563-77.
27. Li, S.; Qin, C.; Cui, S., et al., Discovery of a Natural-Product-Derived Preclinical Candidate for Once-Weekly Treatment of Type 2 Diabetes. *J Med Chem.* **2019,** *62* (5), 2348-2361.
28. Heifetz, A.; Chudyk, E. I.; Gleave, L., et al., The Fragment Molecular Orbital Method Reveals New Insight into the Chemical Nature of GPCR-Ligand Interactions. *J Chem Inf Model.* **2016,** *56* (1), 159-72.
29. Heifetz, A.; Trani, G.; Aldeghi, M., et al., Fragment Molecular Orbital Method Applied to Lead Optimization of Novel Interleukin-2 Inducible T-Cell Kinase (ITK) Inhibitors. *J Med Chem.* **2016,** *59* (9), 4352-63.
30. Mazanetz, M. P.; Ichihara, O.; Law, R. J., et al., Prediction of cyclin-dependent kinase 2 inhibitor potency using the fragment molecular orbital method. *J Cheminform.* **2011,** *3* (1), 2.
31. Fedorov, D. G.; Kitaura, K., Pair interaction energy decomposition analysis. *J Comput Chem.* **2007,** *28* (1), 222-37.
32. Sarver, P.; Acker, M.; Bagdanoff, J. T., et al., 6-Amino-3-methylpyrimidinones as Potent, Selective, and Orally Efficacious SHP2 Inhibitors. *J Med Chem.* **2019,** *62* (4), 1793-1802.
33. Bagdanoff, J. T.; Chen, Z.; Acker, M., et al., Optimization of Fused Bicyclic Allosteric SHP2 Inhibitors. *J. Med. Chem.* **2019,** *62* (4), 1781-1792.
34. LaRochelle, J. R.; Fodor, M.; Ellegast, J. M., et al., Identification of an allosteric benzothiazolopyrimidone inhibitor of the oncogenic protein tyrosine phosphatase SHP2. *Bioorg. Med. Chem.* **2017,** *25* (24), 6479-6485.
35. Garcia Fortanet, J.; Chen, C. H.-T.; Chen, Y.-N. P., et al., Allosteric Inhibition of SHP2: Identification of a Potent, Selective, and Orally Efficacious Phosphatase Inhibitor. *J. Med. Chem.* **2016,** *59* (17), 7773-7782.

Figures

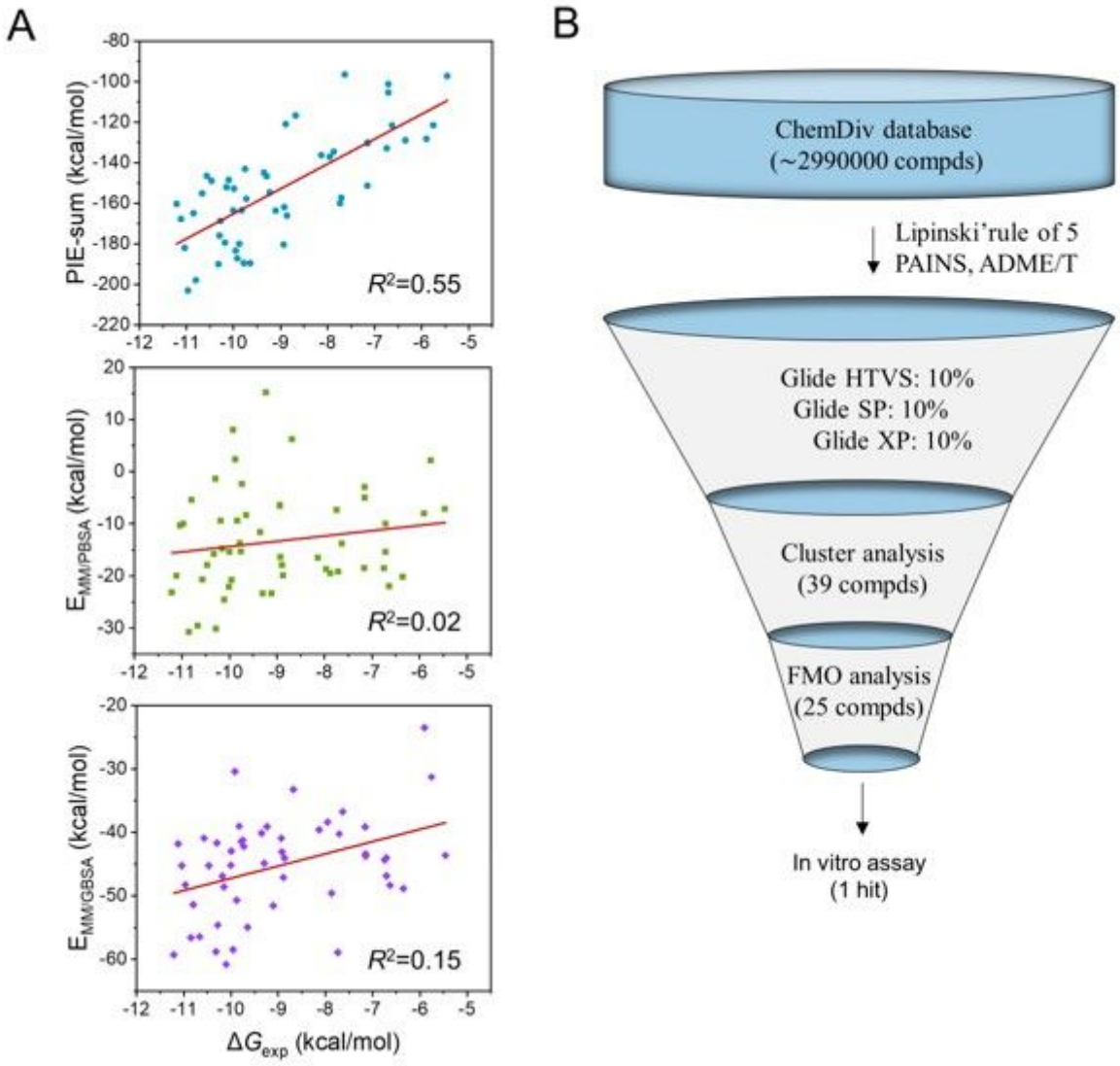

Figure 1

Discovery of a novel SHP2 allosteric inhibitor using the Dock-FMO protocol. (A) Correlations between experimental affinities ($\Delta G_{exp} \approx k_B T \log IC_{50}$) and ΔG values for the reported SHP2 inhibitors predicted by FMO, MM/PBSA, and MM/GBSA, respectively. (B) Workflow for the Dock-FMO virtual screening protocol.

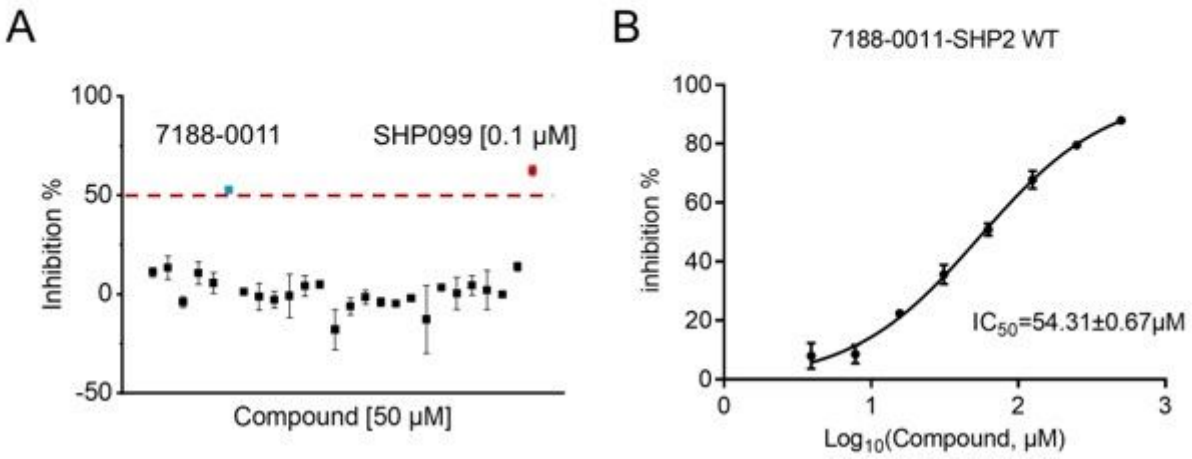

Figure 2

Enzymatic assay of SHP2 allosteric inhibitors *in vitro*. (A) Screening results of candidate compounds on the enzyme activity of SHP2 full length ($SHP2^{WT}$). Red dotted line represents the 50% inhibition threshold for hit identification. Blue dot indicates compound **7188-0011**. Red dot indicates compound **SHP099**, which served as a positive control. The initial screening concentration of the candidate compounds was 50 μM. (B) The dose–response curve of **7188-0011** on SHP2 full length ($SHP2^{WT}$).

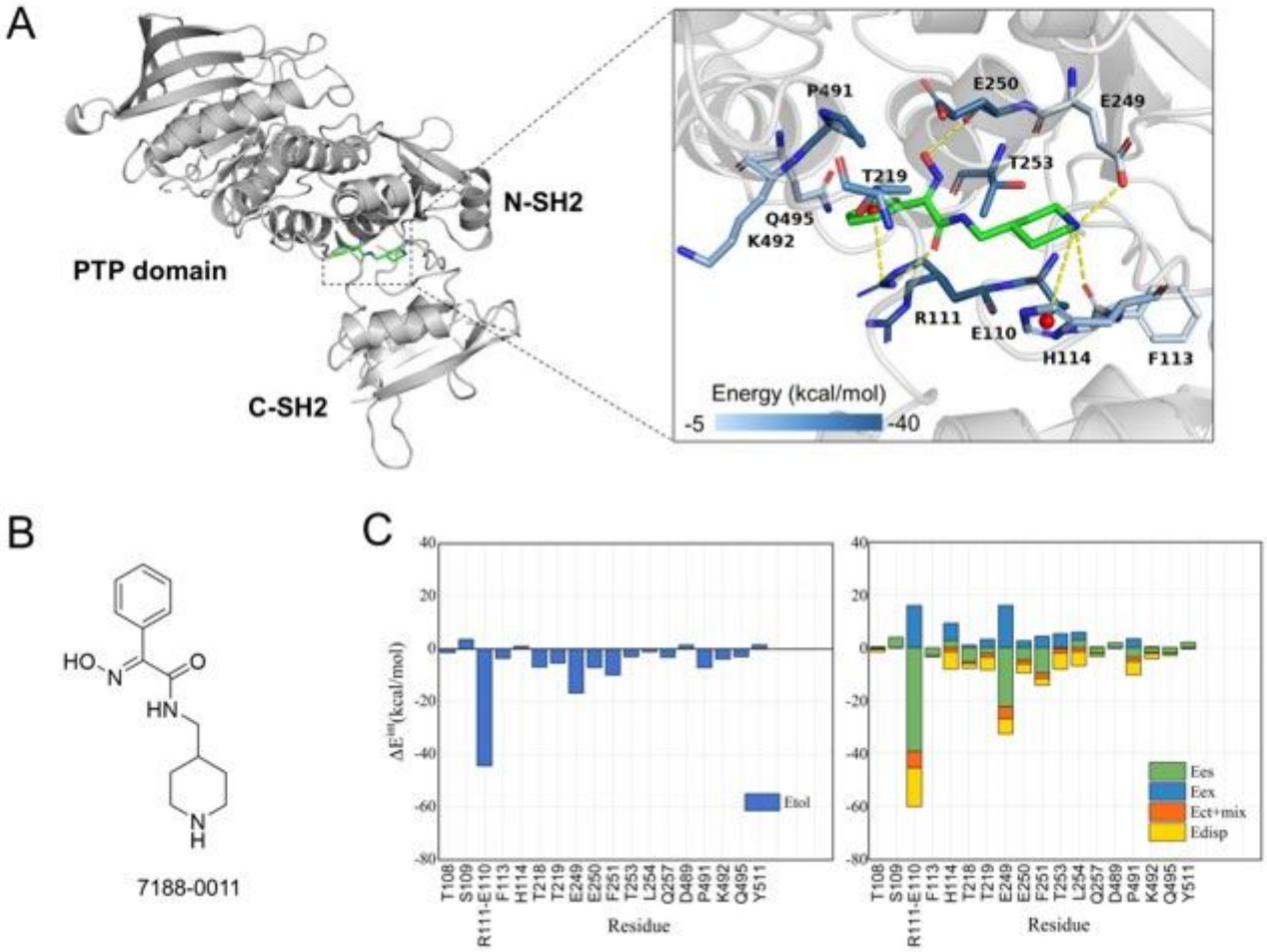

Figure 3

Binding mode prediction and interaction analysis. (A) Predicted binding mode of compound **7188-0011** in the allosteric site of SHP2 (PDB: 5EHR). Hydrogen bonds and salt bridge were depicted as dotted yellow lines. The key residues and the ligand were shown in sticks. The ligand's carbon atoms are shown in green, and carbon atoms of the key residues are colored according to the pair interaction energy (PIE) values calculated using the FMO method. (B) Chemical structure of compound **7188-0011**. (C) The pair interaction energies (PIE) of the compound **7188-0011** and the surrounding residues were drawn on the left graph, and the pair interaction energies decomposition analysis (PIEDA) for these residues was drawn on the right graph. The electrostatic (ES), exchange-repulsion (EX), charge transfer (CT+MIX), and dispersion terms (DI) were represented in green, blue, orange, and yellow, respectively.

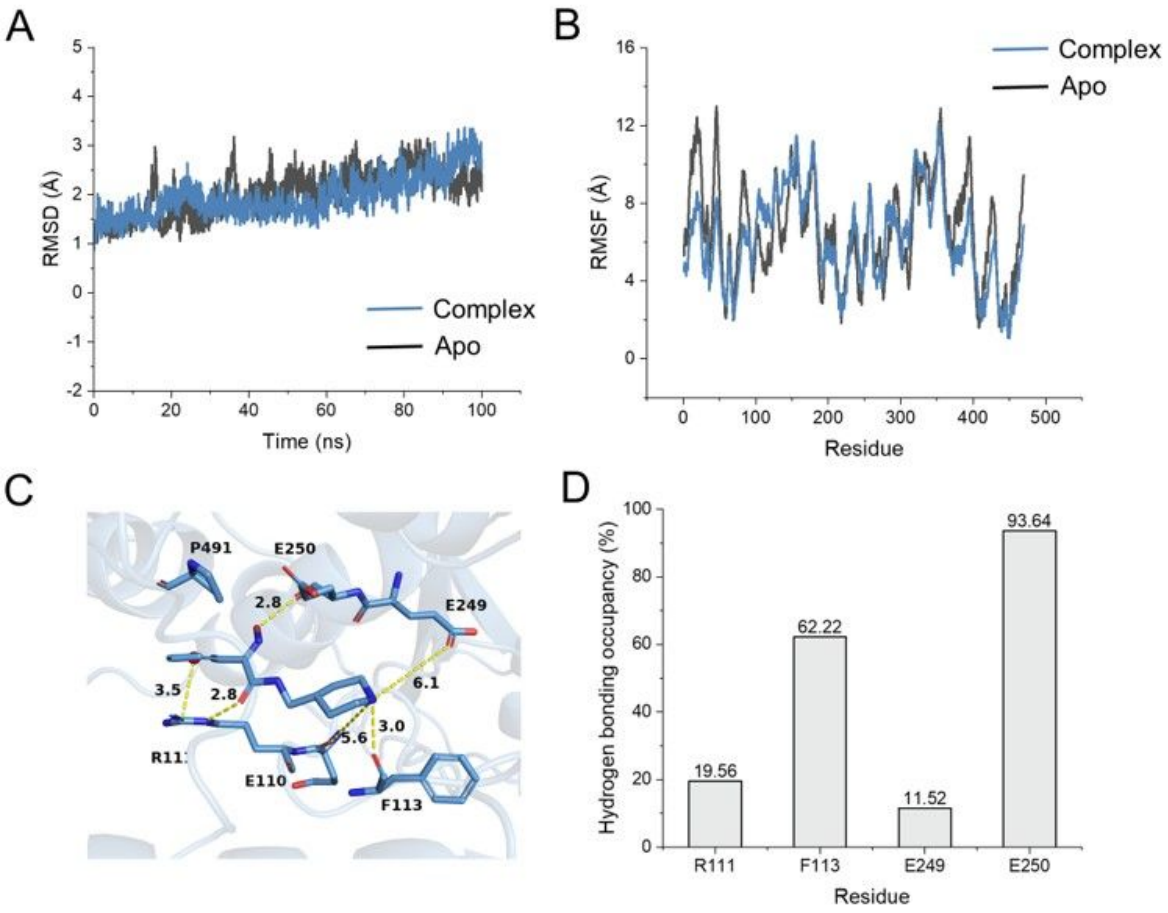

Figure 4

Results of molecular dynamics simulations. (A) The RMSD plots and (B) RMSF plots of the complex and apo protein backbone for 100 ns MD simulations (in blue and black, respectively). (C) The binding mode of the ligand and the surrounding residues in the biggest conformational cluster of 100 ns MD trajectories. Hydrogen bonds and salt bridges were depicted as dotted yellow lines. The key residues and ligand were shown in sticks. (D) The occupancies of hydrogen bonds were represented as bar charts.

Supplementary Files

This is a list of supplementary files associated with this preprint. Click to download.

- Supplementarydata.xlsx
- SupportingInformation.docx